with the needle, at least during the needle elongation stage. To test this, we purified needles from *Y. enterocolitica* incubated in conditions that are either nonpermissive or permissive for secretion (*11*). Under nonpermissive conditions, some YscP was found in the needle fraction as well as in the culture supernatant, whereas under secretion-permissive conditions YscP was found only in the culture supernatant and not in the needle fraction any more (Fig. 4). These data, fitting with previous reports on the localization of YscP (*13*, *14*), show that YscP is associated with newly synthesized needles that are not secreting Yops but not with needles that are secreting Yops.

We propose that YscP controls the length of the needle by acting as a molecular ruler during the stepwise assembly of the injectisome. Because deletions affecting both N- and C-termini of YscP lead to a loss of length control, we hypothesize that the two ends of YscP act as anchors. One end would be attached to the basal body, whereas the other would be connected to the growing tip of the needle. Whatever the anchor mechanism may be, when the needle reaches its mature length, YscP would be fully stretched and signal, via its internal anchor, to the secretion apparatus, which would stop exporting YscF and switch to other substrates. This model (fig. S1) does not contradict the switch function of YscP (*8*, *19*, *20*) but rather includes it in a more complex dual function, which may also exist in some phage tail rulers (*21*). Taking into account the length of 1.9 Å per residue, the ruler domain of YscP would consist of about 300 to 350 residues, leaving more than 150 residues for anchoring and signaling. The fact that YscP is secreted also fits the model, because an internal ruler would be expected to obstruct the 2- to 3-nm-wide secretion channel (*22*). This evokes again the phage tail rulers, which are thought to exit the tail before the tail exerts its function (*21*, *23*). Given the similarity between all the type-III secretion systems (*5*) and the fact that Spa32 (*9*, *10*) InvJ (*24*), and FliK (*25*) are also secreted proteins, it is likely that the mechanism demonstrated here for YscP may apply to the control of the needle length in the other bacteria as well as the length of the flagellar hook. The proposed organization of FliK in three regions—export, hinge$_{(147–265)}$, and switch (*25*)—is also compatible with this view. Finally, the fact that YscP, InvJ, Spa32, and FliK diverged more during evolution than other proteins from type-III secretion suggests that rulers are subjected to fewer constraints. They nevertheless have to share intrinsic properties still to be discovered.

References and Notes

1. G. R. Cornelis, *Nature Rev. Mol. Cell Biol.* **3**, 742 (2002).
2. T. Kubori, A. Sukhan, S. I. Aizawa, J. E. Galan, *Proc. Natl. Acad. Sci. U.S.A.* **97**, 10225 (2000).
3. T. G. Kimbrough, S. I. Miller, *Proc. Natl. Acad. Sci. U.S.A.* **97**, 11008 (2000).
4. A. Blocker *et al.*, *Mol. Microbiol.* **39**, 652 (2001).
5. S. I. Aizawa, *FEMS Microbiol. Lett.* **202**, 157 (2001).
6. R. M. Macnab, *Annu. Rev. Microbiol.* **57**, 77 (2003).
7. T. Hirano, S. Yamaguchi, K. Oosawa, S. Aizawa, *J. Bacteriol.* **176**, 5439 (1994).
8. S. Makishima, K. Komoriya, S. Yamaguchi, S. I. Aizawa, *Science* **291**, 2411 (2001).
9. K. Tamano, E. Katayama, T. Toyotome, C. Sasakawa, *J. Bacteriol.* **184**, 1244 (2002).
10. J. Magdalena *et al.*, *J. Bacteriol.* **184**, 3433 (2002).
11. *Yersinia* builds injectisomes when temperature reaches 37°C, the host temperature. However, Yop secretion is only triggered upon contact with a target cell or artificially by chelating Ca^{2+} ions. The usual procedure consists of growing bacteria at 28°C in oxalated rich medium and then switching the culture to 37°C. In these secretion-permissive conditions, the production of injectisomes is also stimulated. When bacteria are grown at 37°C in the presence of 5 mM Ca^{2+}, they make injectisomes but they do not secrete Yops (nonpermissive conditions). Materials and methods are available as supporting material on *Science* Online.
12. E. Hoiczyk, G. Blobel, *Proc. Natl. Acad. Sci. U.S.A.* **98**, 4669 (2001).
13. I. Stainier *et al.*, *Mol. Microbiol.* **37**, 1005 (2000).
14. P. L. Payne, S. C. Straley, *J. Bacteriol.* **181**, 2852 (1999).
15. For complementation, *yscP* DNA was amplified by polymerase chain reaction and cloned in the pBAD expression vector. Expression was induced with arabinose.
16. I. Katsura, *Nature* **327**, 73 (1987).
17. I. Katsura, R. W. Hendrix, *Cell* **39**, 691 (1984).
18. N. K. Abuladze, M. Gingery, J. Tsai, F. A. Eiserling, *Virology* **199**, 301 (1994).
19. T. Minamino, R. M. Macnab, *J. Bacteriol.* **182**, 4906 (2000).
20. P. J. Edqvist *et al.*, *J. Bacteriol.* **185**, 2259 (2003).
21. M. L. Pedulla *et al.*, *Cell* **113**, 171 (2003).
22. F. S. Cordes *et al.*, *J. Biol. Chem.* **278**, 17103 (2003).
23. R. L. Duda, M. Gingery, F. A. Eiserling, *Virology* **151**, 296 (1986).
24. C. M. Collazo, M. K. Zierler, J. E. Galan, *Mol. Microbiol.* **15**, 25 (1995).
25. T. Minamino, B. Gonzalez-Pedrajo, K. Yamaguchi, S. I. Aizawa, R. M. Macnab, *Mol. Microbiol.* **34**, 295 (1999).

26. We thank M. Duerrenberger for the electron microscopy facility; V. Huschauer for contributing to the needle purification protocol; S. I. Aizawa for advice; M. Kuhn for technical assistance; S. Straley and K. Hughes for supplying *yscP$_{pestisKIM}$* and *Salmonella* LT2; and C. Thompson, U. Jenal, H. Shin, and J. Mota for suggestions. This work was supported by the Swiss National Science Foundation (grant 32-65393.01) and the Swiss Office Fédéral de l'Education et de la Science (European Union Human Potential–Research Training Network CT-2000-00075).

Supporting Online Material

www.sciencemag.org/cgi/content/full/302/5651/1757/DC1
Materials and Methods
Fig. S1
References

11 September 2003; accepted 16 October 2003

Inflammatory Blockade Restores Adult Hippocampal Neurogenesis

Michelle L. Monje, Hiroki Toda, Theo D. Palmer*

Cranial radiation therapy causes a progressive decline in cognitive function that is linked to impaired neurogenesis. Chronic inflammation accompanies radiation injury, suggesting that inflammatory processes may contribute to neural stem cell dysfunction. Here, we show that neuroinflammation alone inhibits neurogenesis and that inflammatory blockade with indomethacin, a common nonsteroidal anti-inflammatory drug, restores neurogenesis after endotoxin-induced inflammation and augments neurogenesis after cranial irradiation.

The birth of new neurons within the hippocampal region of the central nervous system continues throughout life, and the amount of neurogenesis correlates closely with the hippocampal functions of learning and memory (*1*, *2*). The generation of new neurons within the hippocampus is mediated by proliferating neural stem or progenitor cells (NPC) (*3–5*) that are widespread within the adult brain but instructed by local signaling to produce neurons only in discrete areas (*6*, *7*). Alterations in the microenvironment of the stem cell may allow ectopic neurogenesis to occur (*8*, *9*) or even block essential neurogenesis, leading to deficits in learning and memory (*10–12*) such as that observed in patients who receive therapeutic cranial radiation therapy (*13*). In animal models, cranial irradiation ablates hippocampal neurogenesis, in part by damaging the neurogenic microenvironment, leading to a blockade of endogenous neurogenesis (*12*, *13*). Injury induces pro-inflammatory cytokine expression both peripherally and within the central nervous system and induces stress hormones, such as glucocorticoids, that inhibit hippocampal neurogenesis (*10*). The extensive microglial inflammation and release of pro-inflammatory cytokines that accompanies this irradiation-induced failure suggests that inflammatory processes may influence neural progenitor cell activity (*12*, *14*, *15*).

To determine the effects of inflammation on adult hippocampal neurogenesis, we injected bacterial lipopolysaccharide (LPS) into adult female rats to induce systemic inflammation (*16–19*). The intraperitoneal (i.p.) administration of LPS causes a peripheral in-

Stanford University, Department of Neurosurgery, MSLS P309, Mail Code 5487, 1201 Welch Road, Stanford, CA 94305–5487, USA.

*To whom correspondence should be addressed. E-mail: tpalmer@stanford.edu

flammatory cascade that is transduced to the brain via interleukin 1β (IL-1β) from the cerebral vasculature (*16*) and causes a strong up-regulation of central pro-inflammatory cytokine production (*16*, *19*). After LPS exposure, rats were treated systemically with bromo-deoxyuridine (BrdU) for 6 days to label proliferating cells within the hippocampus. Animals were then killed on day 7. The fate of the BrdU-labeled, proliferative cells was analyzed with immunofluorescent staining and confocal microscopy.

Using confocal analysis, we found that peripheral LPS exposure resulted in a 240% increase in the density of activated microglia ($CD68^+/ED1^+$) in the dentate gyrus (Fig. 1, A to C, and F). In normal animals, few $ED1^+$ cells are found. The neuroinflammation achieved in the LPS paradigm was accompanied by a failure to recruit proliferation within the perivascular space, as indicated by an increase in the average distance between dividing cells (Fig. 1, B, C, and H) as well as a 35% decrease in hippocampal neurogenesis (Fig. 1, D, E, and G), as determined by the proportion of nonmicroglial $BrdU^+$ proliferative cells that co-express the early neuronal marker doublecortin (Dcx).

Inflammation in the central nervous system is effectively managed using steroidal anti-inflammatory drugs, yet it is clearly demonstrated in rodents that corticosteroids are potent inhibitors of neurogenesis and their use in the context of augmenting neurogenesis would be strongly contraindicated. To determine whether inflammatory effects could be countered pharmacologically, animals were treated concurrently with a single dose of intraperitoneal LPS and daily doses of the nonsteroidal anti-inflammatory drug (NSAID) indomethacin [2.5 mg/kg, i.p., twice each day]. The effect of peripheral LPS exposure on neurogenesis was completely blocked by systemic treatment with indomethacin, whereas indomethacin alone had no effect on neurogenesis in control animals (Fig. 1, G and H).

Neuroinflammation could inhibit neurogenesis by a variety of mechanisms, including stimulation of the hypothalamic-pituitary-adrenal (HPA) axis with subsequent elevation of glucocorticoids, alterations in the relations between progenitor cells and cells of the neuro-vasculature, or direct effects of activated microglia on the precursor cells. To determine the extent to which microglial activation might directly affect neural stem or progenitor cells, microglia were stimulated in vitro with LPS. LPS is a potent activator of microglia and up-regulates the elaboration of pro-inflammatory cytokines, including interleukin-6 (IL-6) and tumor necrosis factor–α (TNF-α). LPS-stimulated or resting microglia were then co-cultured with normal neural stem cells from the hippocampus under conditions that typically stimulate the differentiation of 30 to 40% of the progenitor cells into immature Dcx-expressing neurons (normalized to a value of 1 in Fig. 2A, control). Neurogenesis in the presence of microglia was assessed as the increase or decrease in Dcx-expressing cells relative to control. Coculture with activated but not resting microglia decreased in vitro neurogenesis to approximately half of control levels (Fig. 2A). LPS added directly to precursor cells had no effect on neurogenesis (*20*).

To determine whether this effect was due to soluble factors or due to cell-cell contact, hippocampal precursor cells were differentiated in the presence of media preconditioned by resting or activated microglia. A similar decrease in neurogenesis was found when precursor cells were exposed to the conditioned medium (CM) from activated microglia (Fig. 2, A and C), indicating that activated microglia produce soluble antineurogenic factors.

Activated microglia produce the potent pro-inflammatory cytokines IL-1β, TNF-α, interferon-γ (INF-γ), and IL-6. Progenitor cells were allowed to differentiate in the presence of each cytokine, and the relative expression of Dcx was scored after 60 hours. Exposure to recombinant IL-6 (50 ng/ml) (Fig. 2, A, D, and E) or to TNF-α (20 ng/ml) (*20*) decreased in vitro neurogenesis by approximately 50%, whereas the effects of IL-1β or INF-γ were not signif-

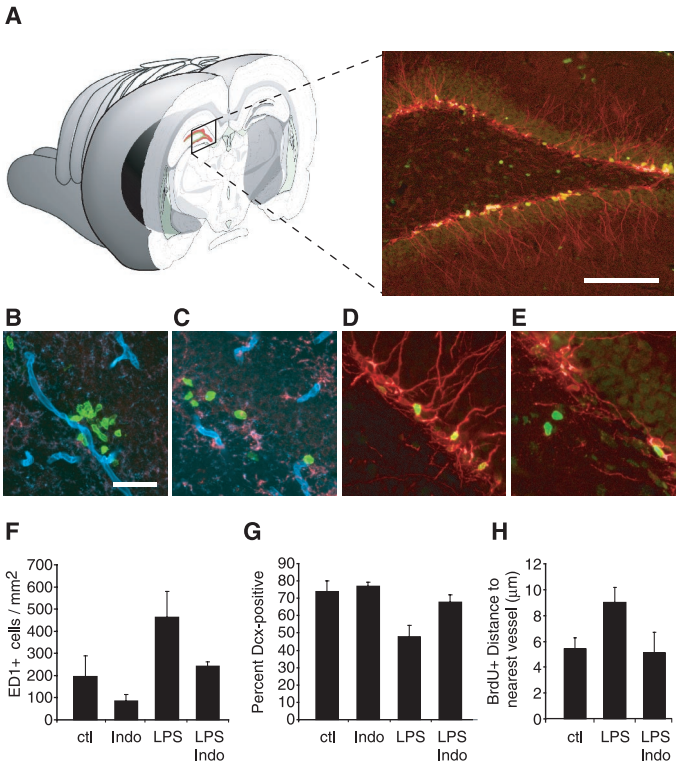

Fig. 1. Inflammation inhibits hippocampal neurogenesis. LPS (1 mg/kg, i.p.) was given to induce a systemic inflammatory response, followed by daily injections of BrdU for 6 days to label proliferating cells. Some rats were given the anti-inflammatory drug indomethacin twice each day (2.5 mg/kg, i.p.) starting concurrently with LPS and continuing for the 1-week paradigm. (**A**) Schematic depicting the anatomic location of the dentate gyrus of the hippocampus within the rodent brain. The neurogenic region of the hippocampus, the granule cell layer, is highlighted in red. To the right, a confocal photomicrograph shows detail of the dentate gyrus stained for the immature neuronal marker Dcx (red) and BrdU for proliferative cells (green). Immature neurons line the subgranule zone at the junction between the granule cell layer and the hilus of the hippocampal dentate gyrus. Bar, 100 μm. (**B** and **C**) Confocal micrographs of vasculature (tomato lectin, blue), BrdU-labeled cells (green), and activated microglia (ED-1, red). Proliferative cells are clustered in large groups proximal to the vasculature in naïve animals (B), but clustering and proximity to the vasculature is decreased in concert with striking activation of microglia after LPS treatment (C). Bar, 30 μm. (**D** and **E**) BrdU-labeled newborn neurons (BrdU, green; Dcx, red) are abundant in naïve animals (D) but are significantly reduced after systemic LPS exposure (E). (**F**) Density of activated microglia ($ED1^+$) in the granule cell layer and subgranule zone. Data are expressed as ED-1 positive cells per mm^2 in a 40-μm section. Systemic LPS exposure significantly increases the density of activated microglia ($P < 0.05$; $n = 3$); treatment with indomethacin decreases this inflammatory response. (**G**) Neuroinflammation induced by systemic LPS inhibits neurogenesis ($P < 0.05$; $n = 3$), as determined by phenotype-specific immunohistochemistry and confocal analysis. Anti-inflammatory therapy with indomethacin restores neurogenesis after LPS exposure ($P < 0.05$; $n = 3$). Data are expressed as the percent of nonmicroglial proliferating cells ($BrdU^+/ED\text{-}1^-$) that co-express Dcx at the end of a 1-week BrdU labeling paradigm. (**H**) Inflammation causes dissociation of the normal relation between proliferating cells and the microvascualture. The average distance from the middle of a $BrdU^+$ nucleus to it nearest tomato lectin–stained vessel was significantly increased in the context of inflammation ($P < 0.05$; $n = 6$); indomethacin restores the vascular association ($P < 0.05$; $n = 3$). Distance measurements were performed on 40-μm sections as measured in the *x* and *y* plane. Proliferating microglia ($BrdU^+/ED\text{-}1^+$) were excluded from the distance measurements.

icant (*20*). Addition of neutralizing anti–IL-6 antibody to CM from activated microglia was able to fully restore in vitro neurogenesis (Fig. 2A). This implicated IL-6 as a key inhibitor of neurogenesis in microglial CM. Although recombinant TNF-α also suppressed neurogenesis, IL-6 blockade alone appeared sufficient to restore neurogenesis in the presence of microglial CM. In contrast to neurogenesis, gliogenesis was unaffected by IL-6 exposure, as indicated by the lack of change in the number of cells expressing the astrocyte [glial fibrillary acidic protein (GFAP)] or early oligodendrocyte (NG2) markers relative to control cultures (Fig. 2E). The hippocampal precursors used here do express the IL-6 receptor, as confirmed by reverse transcriptase–polymerase chain reaction (RT-PCR) (fig. S1).

TUNEL (terminal deoxynucleotidyl transferase–mediated deoxyuridine triphosphate nick end labeling) was used to determine the potential effects of microglial CM or IL-6 on cell death. Microglial CM and IL-6 significantly increased the fraction of TUNEL-positive apoptotic cells in each differentiating culture (control, 0.013 ± 0.007; CM, 0.092 ± 0.023; IL-6, 0.068 ± 0.005; mean ± SEM; $n \geq 3$). Although this increase was substantial, there was no increase in the relative apoptotic index within Dcx^+ versus Dcx^- cells, indicating that cell death was unlikely to select specifically against newborn neurons in vitro (Fig. 2F). The fraction of TUNEL-positive cells that co-labeled with Dcx was 0.92 ± 0.11 for controls (almost all TUNEL-positive profiles are also immunoreactive for Dcx), 0.89 ± 0.07 of TUNEL profiles were Dcx^+ in cultures treated with microglial CM, and 0.83 ± 0.02 (mean ± SEM) in cultures treated with IL-6 (fig. S1).

Mitotic index (fraction of cells labeled with BrdU in 24 hours) in stem cell cultures was unaffected either by CM from stimulated microglia or by IL-6 (92 ± 2.8% in controls versus 95 ± 0.7% in CM or 95 ± 1.7% in IL-6 treated cultures). When the subset of spontaneously forming immature neurons was independently evaluated, there was a subtle but nonsignificant trend to reduced BrdU labeling within the neuronal progeny (88 ± 7.6% in controls versus 82 ± 1.6% in IL-6 treated cultures). Thus, the effect of IL-6 on in vitro neurogenesis appears to induce both a nonspecific decrease in cell survival as well as decreased accumulation of neurons, most likely due to reduced neuronal differentiation rather than selective changes in the proliferation or death of neuroblasts or immature neurons. These findings, taken together with the effect of IL-6 overexpression in transgenic mice (*15*), implicate IL-6 as a potential regulator of hippocampal neurogenesis in neuroinflammation.

Signaling via gp130, the co-receptor of the IL-6 receptor, stimulates the *Notch1* pathway (*21–24*), resulting in an increase in expression of the mammalian homolog of hairy-enhancer-of-split (*Hes 1*) transcription factor (*25*, *26*) and antagonism of pro-neural basic helix-loop-helix (bHLH) genes and hippocampal neurogenesis during development (*27*, *28*). To determine whether IL-6 treatment of adult stem cells leads to an increase in *Hes 1* consistent with the reduction in neuronal cell fate, we performed "real-time" quantitative RT-PCR on total RNA extracted from neural precursors exposed for 60 hours to activated microglial CM or IL-6. Both CM and IL-6 caused a dramatic increase in *Hes1* mRNA expression (3.2- and 7.7-fold increase respectively, relative to control).

Next, we used the irradiation model to determine the relative role of inflammation in this irradiation-induced deficit. Adult rats were treated with indomethacin beginning 2 days before 10 Gray (Gy) cranial irradiation with x-rays (x-irradiation) and continuing daily for 2 months thereafter. Because rats are more radio-resistant than humans, 10 Gy approximates a clinically relevant dose and is below the threshold to cause demyelination or overt vasculopathy in rats (*29–32*). This dose of x-irradiation spares roughly 30% of the NPC proliferative activity but completely ablates the production of neurons (*12*). X-

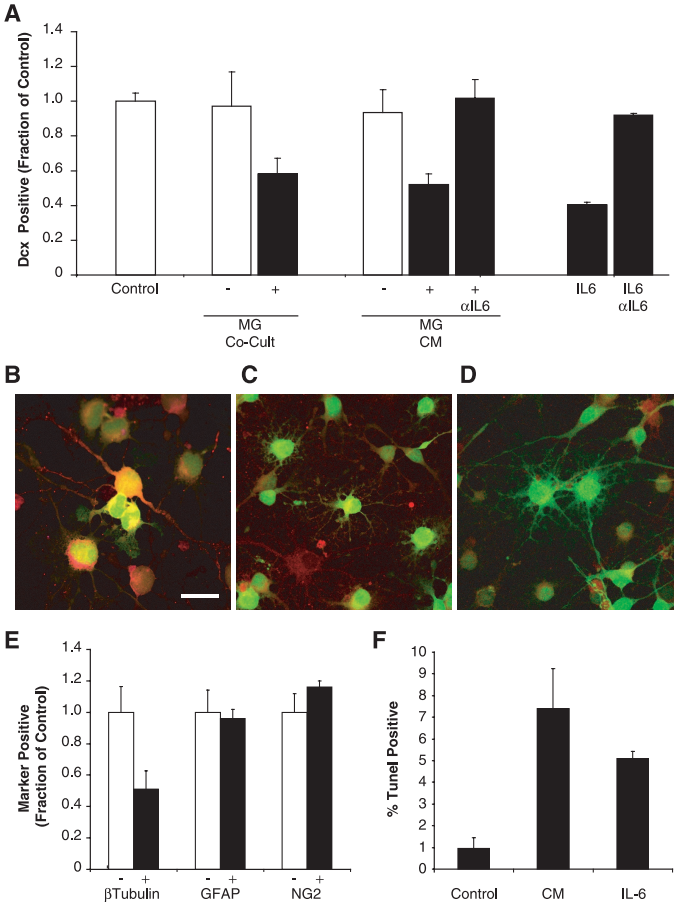

Fig. 2. Activated microglia inhibit neurogenesis via soluble factors that include IL-6. (**A**) Co-culture with microglia (MG), conditioned media (CM) or exposure to recombinant IL-6 decreases neuronal differentiation in vitro. GFP^+ neural progenitor cells (NPCs) were induced to differentiate for 60 hours in the presence or absence of MG that were cultured under nonstimulated conditions (–) or stimulated with LPS for 24 hours before co-culture (+). NPCs were also treated with CM from these same microglial cultures, CM from activated MG pre-mixed with a blocking antibody to IL-6 (αIL6), or recombinant IL-6 in the presence or absence of blocking antibody. Data were collected as the fraction of GFP-expressing cells (NPCs) that co-express the early neuronal marker doublecortin. Co-culture with unstimulated microglia (–MG) had no effect on neuronal differentiation (Student's t test, $P = 0.53$). Co-culture with LPS-stimulated microglia decreased neurogenesis ($P < 0.05$, relative to control or microglial co-culture) as did CM from activated but not resting microglia (Student's t test, $P < 0.05$). A blocking antibody to IL-6 abrogates the CM effects and IL-6 alone (50 ng/ml) reproduced effects of activated microglial CM in reducing neurogenesis ($P < 0.05$; $n = 3$). Data are expressed as the fraction Dcx^+ cells relative to untreated control cultures. (**B** to **D**) Confocal micrographs of representative NPC cultures stained for GFP (green) and Dcx (red). (B) Naïve cells. (C) Cells exposed to conditioned media from activated microglia. (D) Cells exposed to IL-6 (50 ng/ml). Bar, 15 μm. (**E**) Cell fate profile after IL-6 exposure. NPCs were induced to differentiate for 60 hours in the presence of IL-6 (50 ng/ml), and the percentage of cells expressing lineage-specific markers for neurons (type III β-tubulin, βTubulin), astrocytes (GFAP), and immature oligodendrocytes (NG2) was analyzed. Data are expressed as the fraction of cells positive for a given marker normalized to untreated controls. IL-6 caused a significant decrease in the proportion of cells adopting a neuronal fate ($P < 0.05$; $n = 3$), whereas astrogliogenesis and oligogliogenesis were unaffected. (**F**) TUNEL staining in Dcx^+ cells. As in (A), cultures were treated with conditioned medium from LPS-stimulated microglia or treated directly with recombinant IL-6 (50 ng/ml). TUNEL was then scored in the total population, as well as within the subset of cells that had adopted a neuronal phenotype (F). Apoptosis increased significantly overall but not to a larger extent in neurons relative to nonneuronal cells.

irradiation was limited to a 1.5-cm cylinder centered over the cranium (remaining body parts were shielded). One month later, BrdU was administered systemically and, at 2 months after irradiation, brain tissues were analyzed for hippocampal neurogenesis.

As previously reported, (*12*) irradiation caused a striking inflammatory response characterized by the persistence of activated microglia (Fig. 3, A to C) relative to the minimal levels in normal control animals. Unbiased stereologic quantification of $CD68^+/ED1^+$ activated microglia in irradiated animals revealed that indomethacin treatment caused a 35% decrease in activated microglia per dentate gyrus (Fig. 3A). Many of these microglia were proliferative, and a large fraction of all dividing cells within the dentate gyrus were labeled for the monocyte or microglia marker CD11b, which labels both activated and resting microglia (Fig. 3D). A subpopulation of $CD11b^+$ microglia co-expressed the marker NG2 (Fig. 3, C and D; fig. S2), which represents peripheral blood monocytes or microglia that contribute to chronic neuroinflammatory lesions within the brain (*33*, *34*). Indomethacin was particularly effective at decreasing this $CD11b^+/NG2^+$ subpopulation of infiltrating, proliferating peripheral monocytes after irradiation (Fig. 3D), suggesting an indomethacin-induced change in chemokine and/or integrin signaling that recruits transendothelial migration of immune cells after injury.

If inflammation were the primary cause of the lack of neurogenic signaling within the dentate subgranule zone (SGZ), then inflammatory blockade would be expected to restore neurogenesis. Confocal microscopy was used to analyze the proportion of proliferative ($BrdU^+$) cells that co-express markers (Fig. 4A) for mature neurons (NeuN) (Fig. 4B), immature neurons (type III beta tubulin) (Fig. 4C), astrocytes (GFAP) (Fig. 4D), and immature oligodendrocytes ($NG2^+/CD11b^-$) (Fig. 4E). Indomethacin treatment in nonirradiated rats had no effect on cell fate relative to untreated, nonirradiated controls. As previously reported (*12*), irradiation decreased the proportion of proliferative cells adopting a neuronal fate (Fig. 4A). Indomethacin treatment during and after radiation exposure partially restored the relative proportion of proliferative cells adopting a neuronal fate relative to untreated, irradiated animals (37% versus 15%, respectively) (Fig. 4, A to C).

Unbiased stereological quantification of total $BrdU^+$ proliferative cells per neurogenic region [granule cell layer (GCL) plus subgranule zone (SGZ)] of the dentate gyrus revealed no significant difference in overall proliferation between indomethacin-treated and untreated irradiated animals (958 ± 136 proliferative cells versus 828 ± 135 proliferative cells, respectively; control animals exhibited 1938 ± 429 proliferative cells per neurogenic region). Correcting the fraction of proliferative cells adopting a neuronal fate for the total number of proliferative cells yields a significant increase in total newborn hippocampal neurons in indomethacin-treated, irradiated animals compared with untreated, irradiated animals (360 ± 68 newborn neurons versus 125 ± 25 newborn neurons, respectively) (Fig. 4F). This is a substantial increase in neurogenesis but still is only 20% to 25% of the neurogenesis observed in naïve animals (~1600 newborn neurons).

To describe further the relation between microglial inflammation and neurogenesis, we plotted neurogenesis against activated microglial load for each irradiated animal (Fig. 4G). Neurogenesis and inflammation show a striking negative correlation ($R = -0.93$ for activated microglial loads above 1000 per dentate gyrus; activated microglial load was ~500 in controls), suggesting that the extent of inflammation has a direct titrating role on neurogenesis within the adult dentate gyrus.

Our data indicate that inflammation itself can suppress neurogenesis and that chronic inflammation after radiation treatment contributes to the neural stem cell dysfunction that is linked to a progressive postirradiation decline in learning and memory. Chronic microglial activation and peripheral monocyte recruitment with the accompanying increase in local pro-inflammatory cytokine production, including IL-6, emerge as potent antineurogenic components of brain injury. Both IL-6 and the IL-6 receptor-gp130 complex are expressed in the postnatal hippocampus (*19*, *35*), overexpression of IL-6 in the hippocampus suppresses neurogenesis (*15*), and hippocampal expression of the IL-6 receptor increases after systemic challenge with LPS (*19*). IL-6 promotes both astrogliogenesis (*36*) and oligodendrogliogenesis (*37*) and may divert stem cells into a glial program at the expense of neurogenesis after radiation. We find that gliogenesis is relatively well preserved in the irradiated microenvironment (Fig. 4A), and the in vitro data suggests that IL-6 inhibition of neurogenesis is primarily due to a blockade in neuronal differentiation rather than selective influences on cell death or proliferative activity.

Inflammatory blockade with indomethacin decreased microglial activation, accounting for part of the restorative effect of this treatment on neurogenesis after irradi-

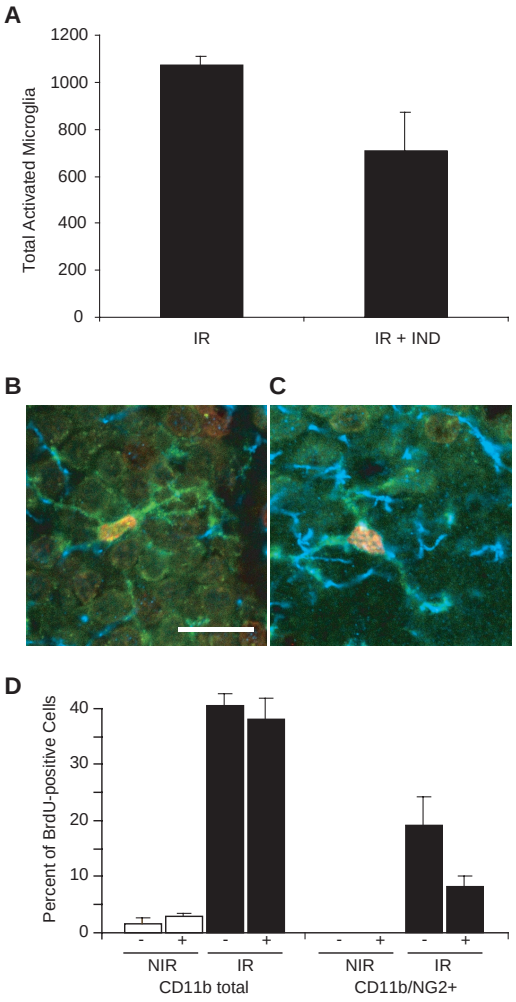

Fig. 3. Indomethacin decreases microglial inflammation after irradiation. Microglial proliferation and activation in nonirradiated (NIR) and irradiated (IR) hippocampi. Indomethacin (IND, ± 2.5 mg/kg) administered orally every 12 hours beginning the day before and for 2 months after irradiation. All groups received BrdU once a day for 6 days starting 4 weeks after irradiation. Animals were killed 2 months after irradiation. (**A**) Unbiased stereologic quantification of ED1-positive activated microglia per dentate gyrus demonstrates that indomethacin reduces the total number of activated (ED1-positive) microglia per dentate gyrus by roughly 35% ($n = 4$ animals per group; Student's t test, $P < 0.05$). (**B** and **C**) Examples of BrdU-labeled (red) microglia (CD11b, green) that are either negative (B) or positive (C) for NG2 (blue). The NG2 epitope is known to be expressed by peripheral monocytes that are recruited into the brain during inflammation (*33*, *34*). Bar, 25 μm. (**D**) Quantification of microglia and invading peripheral monocytes in IR or NIR animals concurrently treated with indomethacin (±). Irradiation caused a dramatic increase in proliferating microglia ($CD11b^+/BrdU^+$ cells) in the granule cell layer and subgranule zone of irradiated animals relative to nonirradiated controls ($n = 4$ animals per group; Student's t test, $P < 0.000001$). Indomethacin had little effect on the relative fraction of BrdU-labeled cells that were microglia after irradiation but significantly reduced the activation state (A) and the relative number of cells that were recruited from the periphery ($NG2^+/CD11b^+$ monocytes, $P < 0.05$, Student's t test; $n = 4$).

ation. However, inflammatory blockade is accompanied by a broad spectrum of effects that could influence neurogenesis in several ways (fig. S3). Restoration of neurogenesis with inflammatory blockade may reduce newborn cell death (*38*) and/or attenuate HPA axis activation (*39*, *40*). The subsequent decrease in pro-inflammatory cytokines and serum glucocorticoid levels may contribute to restored neurogenesis (*41*, *42*). In addition, the microvasculature of the hippocampus is a critical element of the neurogenic microenvironment (*43–45*) and both endotoxin and irradiation-induced inflammation disrupts the association of proliferating progenitor cells with microvessels (*12*). The recruitment of circulating inflammatory cells is highly dependent on the endothelial status and elaboration of chemokines. One of the most robust effects of indomethacin in the present paradigm is the reduction in peripheral monocyte recruitment, suggesting that the inflammatory status of endothelial cells [e.g., expression of chemokines and/or ICAM (intercellular adhesion molecule)] may be normalized by indomethacin. Indeed, one known attribute of indomethacin treatment is the normalization of vascular permeability (*46*), which likely affects the neurogenic vascular microenvironment.

Neuroinflammation and microglial pathology are associated with many diseases of cognition in which memory loss features prominently, such as Alzheimer's Disease, Lewy Body Dementia, and AIDS Dementia Complex (*47–49*). Further, serum IL-6 levels in humans correlate with poor cognitive performance and predict risk of dementia (*50*). Clinical treatment with indomethacin and other NSAIDs ameliorates the risk and/or progression of memory loss (*51*, *52*). Our findings may shed some light on the potential contribution of inflammation-induced neurogenic blockade to memory pathology and on the mechanism of the beneficial effects of NSAID treatment in certain dementias.

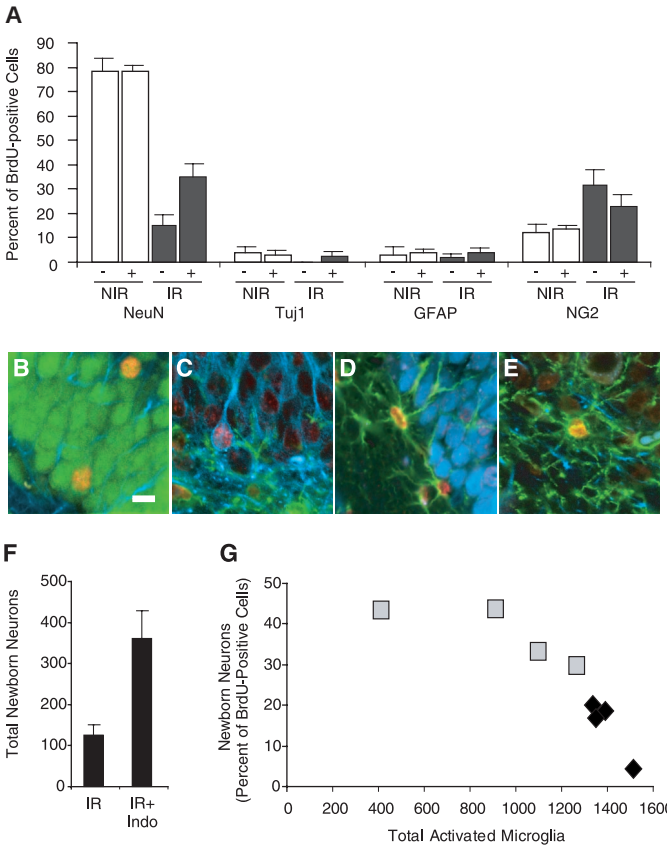

Fig. 4. Anti-inflammatory therapy restores neurogenesis after irradiation. Effect of indomethacin on newborn cells within the SGZ and GCL. NIR, white bars; IR, black bars. Indomethacin (±2.5 mg/kg) was administered orally every 12 hours beginning the day before and for 2 months after irradiation. (**A**) Relative proportion of proliferative cells adopting a recognized cell fate (NeuN, mature neurons; Tuj1, immature neurons; GFAP, astrocytes; $NG2^+/CD11b^-$, immature oligodendrocytes). Data are expressed as means ± SEM; $n = 4$ animals per group. Anti-inflammatory therapy with indomethacin increased the relative proportion of the proliferative cells adopting a neuronal phenotype by 2.5-fold (Student's t test, $P < 0.01$). (**B** to **E**) Representative confocal micrographs of BrdU-labeled (B) mature neurons (NeuN, green; GFAP, blue; BrdU, red), (C) immature neurons (type III β tubulin, blue; NG2, green; BrdU, red); (D) astrocytes (GFAP, green; NeuN, blue); and (E) oligodendrocytes (NG2, green, CD11b, blue; BrdU, red). Bars, 10 μm. (**F**) Increase in total number of newborn neurons per GCL plus SGZ in irradiated animals treated with indomethacin. Unbiased stereologic quantification of $BrdU^+$ cells adjusted for fraction of $BrdU^+$ cells adopting a neuronal phenotype ($NeuN^+$ plus $Tuj1^+$). IR, irradiated; IR+Indo, irradiated, indomethacin treated. Anti-inflammatory therapy substantially increases the absolute number of newborn neurons per hippocampus (Student's t test, $P < 0.01$). (**G**) Inflammation negatively correlates with the accumulation of new neurons. The fraction of dividing cells adopting a neuronal phenotype is inversely proportional to total number of activated microglia per dentate gyrus. Each data point represents one irradiated animal. Control irradiated animals, black diamonds; indomethacin-treated irradiated animals, gray squares.

References and Notes

1. T. J. Shors *et al.*, *Nature* **410**, 372 (2001).
2. R. Feng *et al.*, *Neuron* **32**, 911 (2001).
3. H. A. Cameron, R. McKay, *Curr. Opin. Neurobiol.* **8**, 677 (1998).
4. F. H. Gage, G. Kempermann, T. D. Palmer, D. A. Peterson, J. Ray, *J. Neurobiol.* **36**, 249 (1998).
5. T. D. Palmer, J. Takahashi, F. H. Gage, *Mol. Cell Neurosci.* **8**, 389 (1997).
6. J. O. Suhonen, D. A. Peterson, J. Ray, F. H. Gage, *Nature* **383**, 624 (1996).
7. M. B. Luskin, *J. Neurobiol.* **36**, 221 (1998).
8. H. Nakatomi *et al.*, *Cell* **110**, 429 (2002).
9. S. S. Magavi, B. R. Leavitt, J. D. Macklis, *Nature* **405**, 951 (2000).
10. H. A. Cameron, P. Tanapat, E. Gould, *Neuroscience* **82**, 349 (1998).
11. T. M. Madsen, P. E. Kristjansen, T. G. Bolwig, G. Wortwein, *Neuroscience* **119**, 635 (2003).
12. M. L. Monje, S. Mizumatsu, J. R. Fike, T. D. Palmer, *Nature Med.* **8**, 955 (2002).
13. M. L. Monje, T. Palmer, *Curr. Opin. Neurol.* **16**, 129 (2003).
14. N. Picard-Riera *et al.*, *Proc. Natl. Acad. Sci. U.S.A.* **99**, 13211 (2002).
15. L. Vallieres, I. L. Campbell, F. H. Gage, P. E. Sawchenko, *J. Neurosci.* **22**, 486 (2002).
16. N. P. Turrin *et al.*, *Brain Res. Bull.* **54**, 443 (2001).
17. K. N. Shaw, S. Commins, S. M. O'Mara, *Behav. Brain Res.* **124**, 47 (2001).
18. S. Terrazzino, A. Bauleo, A. Baldan, A. Leon, *J. Neuroimmunol.* **124**, 45 (2002).
19. L. Vallieres, S. Rivest, *J. Neurochem.* **69**, 1668 (1997).
20. M. Monje, H. Toda, T. D. Palmer, data not shown.
21. A. Chojnacki, T. Shimazaki, C. Gregg, G. Weinmaster, S. Weiss, *J. Neurosci.* **23**, 1730 (2003).
22. L. S. Wright *et al.*, *J. Neurochem.* **86**, 179 (2003).
23. K. Nakashima, T. Taga, *Mol. Neurobiol.* **25**, 233 (2002).
24. P. Marz, K. Heese, B. Dimitriades-Schmutz, S. Rose-John, U. Otten, *Glia* **26**, 191 (1999).
25. M. Ishibashi *et al.*, *EMBO J.* **13**, 1799 (1994).
26. M. Ishibashi *et al.*, *Genes Dev.* **9**, 3136 (1995).
27. P. Castella, J. A. Wagner, M. Caudy, *J. Neurosci. Res.* **56**, 229 (1999).
28. Y. Nakamura *et al.*, *J. Neurosci.* **20**, 283 (2000).
29. H. Hodges *et al.*, *Behav. Brain Res.* **91**, 99 (1998).
30. W. Calvo, J. W. Hopewell, H. S. Reinhold, T. K. Yeung, *Br. J. Radiol.* **61**, 1043 (1988).
31. G. E. Sheline, W. M. Wara, V. Smith, *Int. J. Radiat. Oncol. Biol. Phys.* **6**, 1215 (1980).
32. J. E. Marks, R. J. Baglan, S. C. Prassad, W. F. Blank, *Int. J. Radiat. Oncol. Biol. Phys.* **7**, 243 (1981).
33. J. Bu, N. Akhtar, A. Nishiyama, *Glia* **34**, 296 (2001).
34. L. L. Jones, Y. Yamaguchi, W. B. Stallcup, M. H. Tuszynski, *J. Neurosci.* **22**, 2792 (2002).
35. D. Watanabe *et al.*, *Eur. J. Neurosci.* **8**, 1630 (1996).
36. N. J. Van Wagoner, E. N. Benveniste, *J. Neuroimmunol.* **100**, 124 (1999).
37. A. Valerio *et al.*, *Mol. Cell Neurosci.* **21**, 602 (2002).
38. C. T. Ekdahl, J. H. Classen, S. Bonde, Z. Kokaia, O. Lindvall, *Proc. Natl. Acad. Sci. U.S.A.* 10.1073/pnas.2234031100 (2003).
39. F. Shintani *et al.*, *J. Neurosci.* **15**, 1961 (1995).
40. T. M. Reyes, C. L. Coe, *Am. J. Physiol.* **274**, R139 (1998).
41. E. Gould, B. S. McEwen, P. Tanapat, L. A. Galea, E. Fuchs, *J. Neurosci.* **17**, 2492 (1997).
42. P. Tanapat, L. A. Galea, E. Gould, *Int. J. Dev. Neurosci.* **16**, 235 (1998).
43. C. Leventhal, S. Rafii, D. Rafii, A. Shahar, S. A. Goldman, *Mol. Cell Neurosci.* **13**, 450 (1999).
44. A. Louissaint Jr., S. Rao, C. Leventhal, S. A. Goldman, *Neuron* **34**, 945 (2002).
45. T. D. Palmer, A. R. Willhoite, F. H. Gage, *J. Comp. Neurol.* **425**, 479 (2000).
46. H. R. Reichman, C. L. Farrell, R. F. Del Maestro, *J. Neurosurg.* **65**, 233 (1986).
47. D. W. Dickson, *Clin. Geriatr. Med.* **17**, 209 (2001).
48. I. R. Mackenzie, *Neurology* **55**, 132 (2000).
49. B. J. Brew, *Neurol. Clin.* **17**, 861 (1999).
50. J. D. Weaver *et al.*, *Neurology* **59**, 371 (2002).
51. J. Rogers *et al.*, *Neurology* **43**, 1609 (1993).
52. B. A. in t' Veld *et al.*, *N. Engl. J. Med.* **345**, 1515 (2001).

53. We thank T. Wyss-Coray for his gift of BV-2 microglial cells; B. E. Hoyte for help with manuscript graphics; R. Malenka for use of the Pritzker Foundation confocal microscope; B. D. Hoehn and S. P. K. Samagh for technical assistance; and S. K. McConnell, W. C. Mobley, M. Tessier-Lavigne D. Schall, O. Mitrasinovic and P. G. Fisher for valuable insights. We would also like to thank C. Ekdahl, Z. Kokaia, and O. Lindvall and colleagues for their helpful discussion of parallel findings in models of epilepsy. Supported by grants MH20016-05 from the National Institutes of Mental Health, F30 NS04696701 from the National Institutes of Neurological Disorders and Stroke, and Palmer Lab Start up funds from the Department of Neurosurgery, Stanford University.

Supporting Online Material
www.sciencemag.org/cgi/content/full/1088417/DC1
Materials and Methods
Figs. S1 to S3
References

25 June 2003; accepted 26 September 2003
Published online 13 November 2003;
10.1126/science.1088417
Include this information when citing this paper.

Spatiotemporal Rescue of Memory Dysfunction in *Drosophila*

Sean E. McGuire,[1] Phuong T. Le,[1] Alexander J. Osborn,[3] Kunihiro Matsumoto,[4] Ronald L. Davis[1,2]*

We have developed a method for temporal and regional gene expression targeting (TARGET) in *Drosophila* and show the simultaneous spatial and temporal rescue of a memory defect. The transient expression of the *rutabaga*-encoded adenylyl cyclase in the mushroom bodies of the adult brain was necessary and sufficient to rescue the *rutabaga* memory deficit, which rules out a developmental brain defect in the etiology of this deficit and demonstrates an acute role for *rutabaga* in memory formation in these neurons. The TARGET system offers general utility in simultaneously addressing issues of when and where gene products are required.

Memory traces are typically thought to manifest as plastic changes in neuronal physiology that occur in specific regions of the brain. In *Drosophila*, distinct brain structures known as the mushroom bodies have been demonstrated to have an important role in the associative learning and memory of olfactory stimuli (*1*–*6*); however, the location of olfactory memory acquisition and storage in the *Drosophila* brain has remained unknown. One strategy for identifying the brain regions in which plasticity is required for the establishment of memory traces is to target the expression of a gene thought to be required for neuronal plasticity to specific regions of the brain in an animal mutant for that gene, using the GAL4/UAS system (*6*, *7*).

However, a critical question when using this approach is whether memory rescue represents the rescue of a physiological defect in the neurons themselves or of a defect in the proper development of the animal's nervous system. The expression of the *rutabaga*-encoded type I adenylyl cyclase in the mushroom bodies during development and adulthood is sufficient to rescue the short-term memory defect in *rutabaga* mutant flies, suggesting that the memory trace might localize to the mushroom bodies (*6*). The GAL4 elements that were used in these experiments, however, drive expression in both the developing and adult mushroom bodies and, therefore, did not distinguish between a developmental and adult requirement for *rutabaga* for memory rescue. The ability to distinguish between a developmental defect in neuronal connectivity and a physiological defect in neuronal plasticity is crucial for understanding the implications of behavioral rescue experiments for the localization of a memory trace.

This distinction is particularly relevant in the case of type I adenylyl cyclases. Type I adenylyl cyclases are required for some forms of synaptic plasticity and memory (*8*). As a class, they respond synergistically to intracellular calcium and heterotrimeric GTP-binding protein signaling, thus representing a potential molecular substrate for the detection and integration of the coincidence between a conditioned stimulus and an unconditioned stimulus on a neuron (*9*–*11*). However, the type I adenylyl cyclases also have well-known roles in neural development. The mouse mutant *barrelless*, which lacks barrels in the primary somatosensory cortex and exhibits defects in the patterning of this brain region in the early postnatal stage (*12*), results from a mutation in type I adenylyl cyclase (*13*). In *Drosophila*, defects in the development of the mushroom bodies have been observed in *rutabaga* mutants, including a possible reduction in the number of axonal tracts (*14*), a reduction in the volume of their dendritic arbors (*15*), and defects in the structural plasticity of the mushroom bodies in response to developmental conditions (*16*). These observations suggest that *rutabaga* is potentially required for the normal development of the mushroom bodies.

We developed a technology that allows for both temporal and regional gene expression targeting (TARGET) in *Drosophila* using the conventional GAL4/UAS system (Fig. 1A) (*17*). The traditional GAL4/UAS system provides tight regional control of gene expression, but it lacks experimenter-defined temporal control and, hence, does not enable a systematic study of the critical time periods in which the expression of a transgene is required in a specific tissue for a particular phenotype. We therefore cloned a temperature-sensitive version of the GAL80 protein (GAL80ts), which normally functions as a repressor of GAL4 in yeast, and tested it for temperature-sensitive regulation of GAL4 activity in both yeast and *Drosophila* (*18*).

We first tested the ability of GAL80ts to repress GAL4-induced expression in the brains of adult flies. Fig. 1B, panels *i* and *ii*, demonstrates the fluorescence pattern of green fluorescent protein expression in the brains of adult flies that carry the GAL4 driver c739, which drives expression at high levels in the α and β lobes of the mushroom bodies (*3*, *19*). Flies were raised at 19°C and were either untreated (–hs, *i*) or treated (+hs, *ii*) with a 12-hour exposure to 30°C. In the absence of heat shock, flies that also expressed GAL80ts from the tubulin 1α promoter showed undetectable levels of GFP fluorescence in the brain (Fig. 1B, *iii*), whereas flies treated with the heat pulse regimen showed increased levels of GFP fluorescence in the mushroom bodies (Fig. 1B, *iv*). Flies expressing wild-type GAL80 from the tubulin 1α promoter showed no GFP fluorescence in either the untreated or treated groups (Fig. 1B, *v* and *vi*). Flies raised at 25°C carrying $GAL4^{c739}$ along with GAL80ts and the UAS-GFP reporter showed faint but detectable levels of GFP fluorescence.

We next measured GFP mRNA levels by reverse transcription–polymerase chain reaction (RT-PCR) in flies after their exposure to varying lengths of heat shock. Expression of GFP was detected as early as 30 min into the heat shock. After 3 hours at 32°C, the GFP

[1]Department of Molecular and Cellular Biology, [2]Department of Psychiatry and Behavioral Sciences, [3]Department of Molecular & Human Genetics, Baylor College of Medicine, Houston, TX 77030, USA. [4]Department of Molecular Biology, Graduate School of Science, Nagoya University, Nagoya 464–8602, Japan.

*To whom correspondence should be addressed. E-mail: rdavis@bcm.tmc.edu